

Additive Manufacturing Data Analytics



Drew Burky, Jan Dee, & Eric Vo

Background

Current State: Analyze how differences in powder bed fusion processing conditions affect the microstructure and mechanical properties of Ti6Al4V alloy parts. Current analysis of microstructure, such as SEM and EBSD are destructive and expensive in terms of time and effort.



Figure 1.1: Real, titanium alloy additive manufactured test coupon

Main Objective: Find a way to predict final microstructure from different laser input parameters and melt pool data.

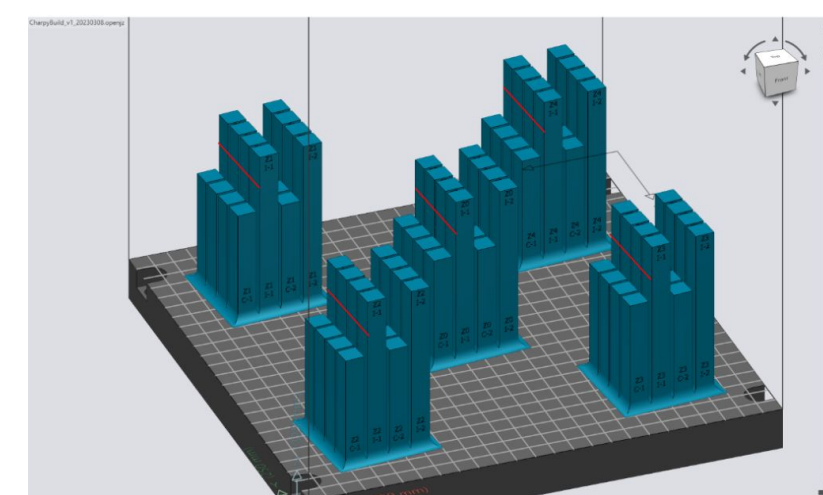


Figure 1.2: 3D render of the test build for melt pool data

Methodology & Resources

Methodology:

We use parametric runs with different laser input parameters analyze the liquid to solid transition data produced and make conclusions on the final microstructure. For the melt pool, we analyze the layers to look for potential anomalies, and examine a 1mm square to compare the distributions to simulation data.

Resources Used:

Cubit (mesh generation), Truchas (simulation), Paraview (visualization)

References & Acknowledgements

Wei, H. L.; Mukherjee, T.; Zhang, W.; Zuback, J. S.; Knapp, G. L.; De, A.; DebRoy, T. Mechanistic Models for Additive Manufacturing of Metallic Components. *Progress in Materials Science* 2021, 116, 100703. <https://doi.org/10.1016/j.pmatsci.2020.100703>.

Special thanks to our Mentors: Rob Grube (Boeing), Naren Raghavan (Boeing), Luna Huang (UW), Rick Schleusener (UW)

Melt Pool

Visualization

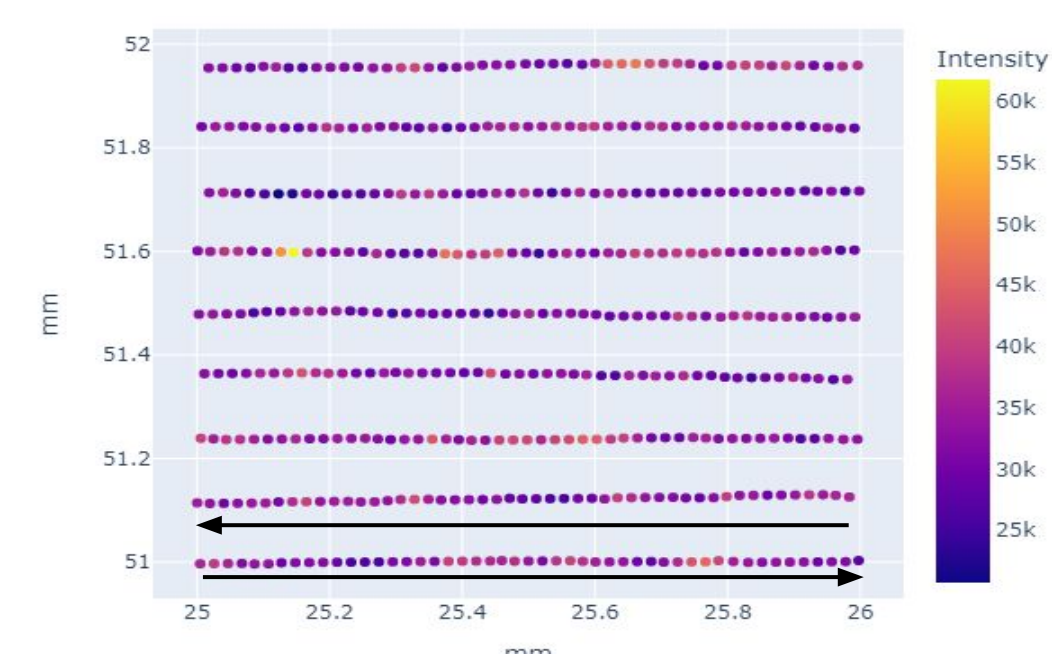


Figure 2.1: Path of melt pool intensity through real build

Analysis

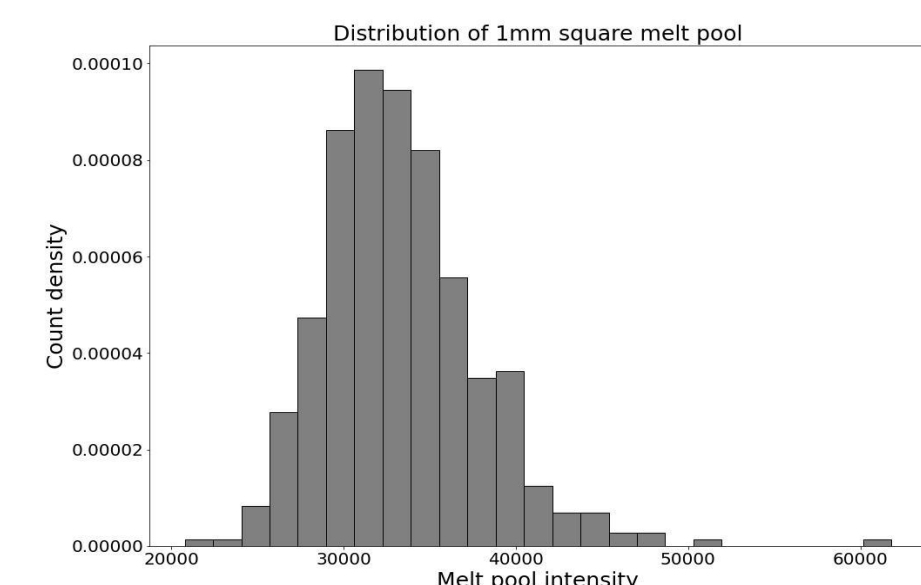


Figure 2.3: Distribution of melt pool intensity over 1mm square

Simulation

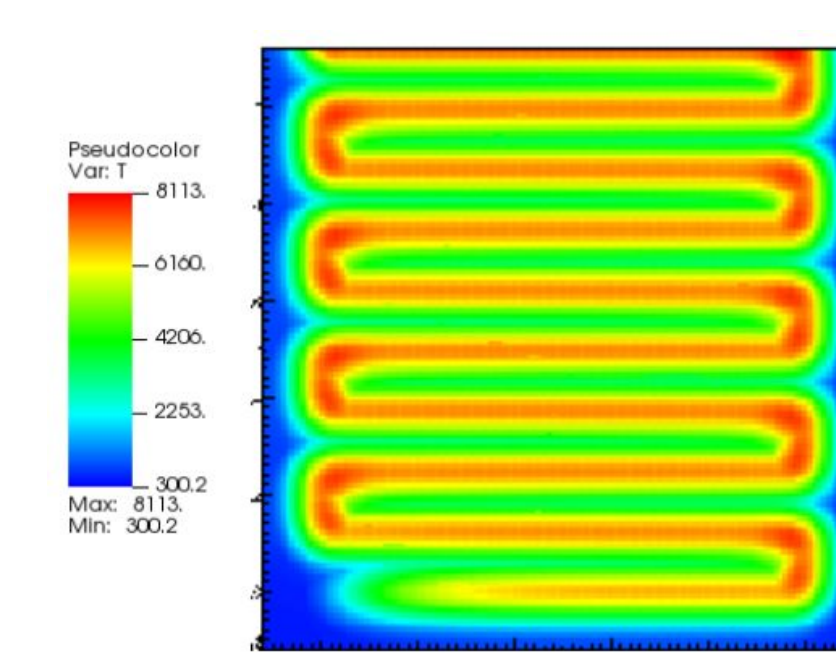


Figure 2.2: Simulation raster pattern of laser with 340W, 1.25 m/s velocity

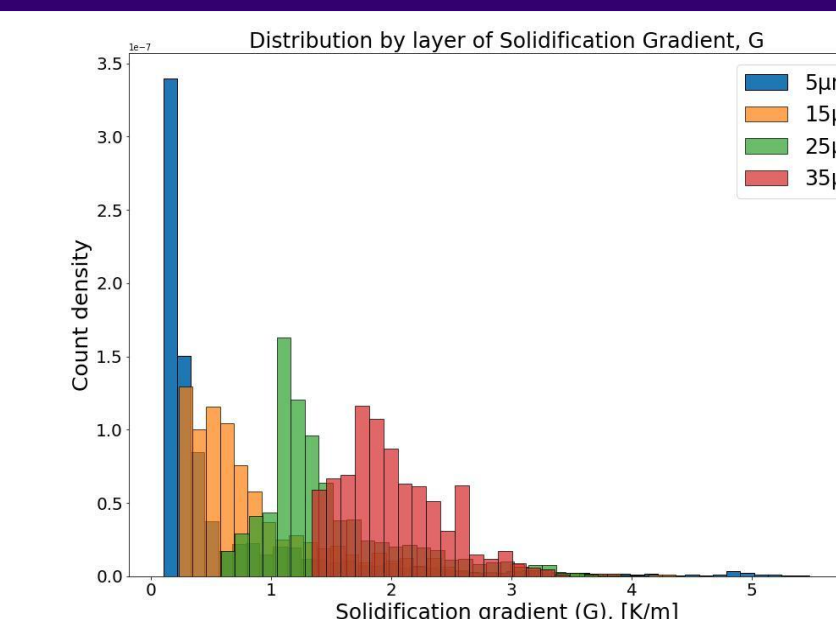


Figure 2.4: Distribution of solidification gradient on different layers of simulation

Discussion, Conclusion, & Future Work

As seen in figure 2.2, the simulation is able to accurately mimic the laser, creating a raster pattern with the same hatch spacing as the melt pool in figure 2.1. With this, the distributions can be compared to understand the differences in layers of simulation data, The melt pool intensity distribution as shown in figure 2.3 follows a gaussian distribution.

For the different simulation outputs, most notable for the solidification gradient (G), the distribution greatly differs for each simulated layer as shown in figure 2.4. Further analysis and additional datasets for better are needed in order to establish better connection between melt pool and simulation.

Parametric Simulation Regression

Table 1: Parametric Run Conditions

| Laser Power (W) | Velocity (mm/s) | Output_T | Hatch Spacing (mm) | Energy Density (J/mm ³) |
|-----------------|-----------------|----------|--------------------|-------------------------------------|
| 340 | 1250 | 0.0094 | 0.12 | 2.2667 |
| 170 | 625 | 0.0187 | | |
| 226.6 | 833.3 | 0.0140 | | |
| 281.1 | 1033.3 | 0.0113 | | |
| 340.0 | 1087.0 | 0.0108 | 0.12 | 2.6067 |
| 170.0 | 543.5 | 0.2153 | | |
| 226.6 | 724.6 | 0.0161 | | |
| 281.1 | 898.6 | 0.0130 | | |
| 340.0 | 961.5 | 0.0122 | 0.12 | 2.9467 |
| 170.0 | 480.8 | 0.0243 | | |
| 226.6 | 641.0 | 0.0183 | | |
| 281.1 | 794.9 | 0.0147 | | |
| 340.0 | 1470.6 | 0.0080 | 0.12 | 1.9267 |
| 170.0 | 735.3 | 0.0159 | | |
| 226.6 | 980.3 | 0.0119 | | |
| 281.1 | 1212.7 | 0.0096 | | |
| 340.0 | 1785.7 | 0.0066 | 0.12 | 1.5867 |
| 170.0 | 892.9 | 0.0131 | | |
| 226.6 | 1190.4 | 0.0098 | | |
| 281.1 | 1476.2 | 0.0079 | | |

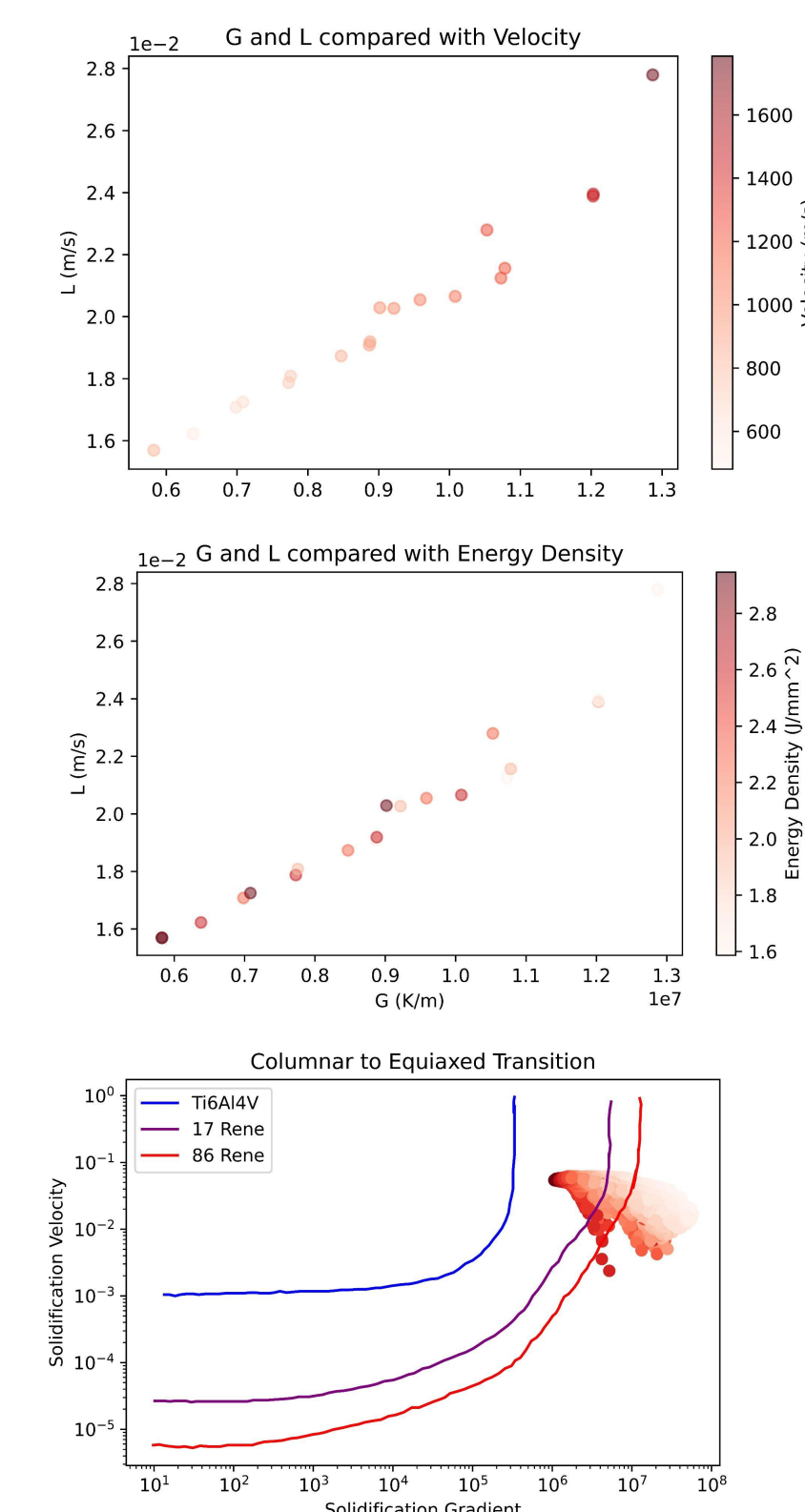


Figure 3: Parametric runs of simulation organized by velocity and predicted microstructure

Discussion & Conclusion & Future work

As seen in the first and second plots, the solidification gradient and velocity are more strongly correlated to the laser's velocity, rather than the energy density on the overall build.

By creating a set of 20 simulation runs with two independent variables we are able to make a regression model which correlates solidification data with laser power and velocity with a R_squared value of 0.925.

The last plot shows a projection of the results of solidification data onto literature values of 3 titanium alloys, Ti 6-4 powder, and with increasing additions of nickel alloy. The results of our simulations can be interpreted in this way, where our strongest laser signals are columnar on the Ti64 phase diagram, but may show equiaxed behavior in other compositions.